An Automatic R and T peak Detection Method Based on the Combination of Hierarchical Clustering and Discrete Wavelet Transform

Hanjie Chen, *Student Member, IEEE,* and Koushik Maharatna, *Member, IEEE,*

***Abstract*—The detection and delineation of QRS-complexes and T-waves in Electrocardiogram (ECG) is an important task because these features are associated with the cardiac abnormalities including ventricular arrhythmias that may lead to sudden cardiac death. In this paper, we propose a novel method for the R-peak and the T-peak detection using hierarchical clustering and Discrete Wavelet Transform (DWT) from the ECG signal. In the first step, a template of the single ECG beat is identified. Secondly, all R-peaks are detected by using hierarchical clustering. Then, each corresponding T-wave boundary is delineated based on the template morphology. Finally, the determination of T wave peaks is achieved based on the Modulus-Maxima Analysis (MMA) of the DWT coefficients. We evaluated the algorithm by using all records from the MIT-BIH arrhythmia database and QT database. The R-peak detector achieved a sensitivity of 99.89%, a positive predictivity of 99.97% and 99.83% accuracy over the validation MIT-BIH database. In addition, it shows a sensitivity of 100%, a positive predictivity of 99.83% in manually annotated QT database. It also shows 99.92% sensitivity and 99.96% positive predictivity over the automatic annotated QT database. In terms of the T-peak detection, our algorithm is verified with 99.91% sensitivity and 99.38% positive predictivity in manually annotated QT database.**

***Index Terms*—ECG; R and T peak detection; Hierarchical clustering; DWT.**

.

I. Introduction

ACCORDING to the World Health Organization (WHO), 31% of all global deaths are due to the Cardiovascular Diseases (CVDs) [1]. Diagnosising CVDs and ensuring the patients can receive appropriate treatment are necessary to prevent premature deaths. The analysis of the ECG is widely applied in the diagnosis of these heart disorders [2]. The most useful information in the ECG is normally derived from the amplitudes and intervals of these dividual waves that are defined by the fiducial points (e.g. onset, offset, peak). In general, these features are used to classify the normal and abnormal heartbeats in this process of diagnosis of a specific heart disease, e.g. congestive heart failure (CHF) [3] and cardiac arrhythmia [4]. Therefore, it is necessary to extract various features of ECG in order to diagnose the heart diseases. Among the ECG wave, the QRS complex is relatively easy to identify because of its specific morphology and high amplitude. However, the T-wave delineation is a more challenging task, due to its low amplitude and possibly irregular morphology. In addition, noises such as baseline wandering and power line interference are main factors that can result in faulty T-wave delineation.

Over the decade, a number of automated algorithms have been developed for ECG delineation. In general, there are two main groups of ECG feature extraction algorithms, which are QRS detection and non-QRS delineation algorithms [5]. The first QRS detection algorithm was introduced by Pan and Tompkins [6]. There are other attempts for QRS detection based on shannon energy envelope (SEE) [7], wavelet transform (WT) [8]–[12], phase-space reconstruction (PSR) [13], Optimized adaptive thresholding [14], iterative state machines [15], and moving-average filters [16]. Concerning the non-QRS delineation algorithms, the main objective is to determine the peaks and boundaries of the individual QRS complexes, P and T waves. The existing literature on ECG wave delineation algorithms is extensive and focuses particularly on frequency aspect, e.g. DWT [17] [18], the combination of wavelet transform and hybrid hidden Markov models [19]. Among other popular methods, the phasor transform [20], moving-average filters [21], [22], morphological mathematical filtering with Elgendi's algorithm [23] and the correlation analysis-based method [24] have also been applied to detect ECG fiducial points.

However, the major concern associated with these algorithms is their detection accuracy, more importantly low positive predictivity ($+P$) caused by the large number of false-positives (FPs) of R-peak detection. In addition, current methods can be error-prone, especially cannot achieve satisfactory performance for T-wave detection due to the variable morphology of the T-wave [25]. This is particularly important in Implantable Cardioverter Defibrillator (ICD) device where depending upon the detected R-R interval, a patient's heart is given high-voltage electrical shock if necessary. In this context, even more severe problem is the T-wave oversensing phenomenon, where T-peak is misidentified as an R-peak resulting into a wrong R-R interval calculation. This leads to a delivery of an electrical shock even though the patient's heart rhythm is normal. Inspired by this fact, a novel automated ECG feature extraction algorithm based on the hierarchical clustering and discrete wavelet transform, which is specifically designed to detect R-peak and T-peak is proposed in this paper. The hierarchical clustering method is used to identify the

Hanjie Chen is with the University of Southampton, School of Electronics and Computer Science, Southampton SO17 1BJ, UK e-mail: (hc4y15@soton.ac.uk).

Koushik Maharatna is with the University of Southampton, School of Electronics and Computer Science, Southampton SO17 1BJ, UK e-mail: (km3@ecs.soton.ac.uk).

This article has been accepted for publication in a future issue of this journal, but has not been fully edited. Content may change prior to final publication. Citation information: DOI 10.1109/JBHI.2020.2973982, IEEE Journal of Biomedical and Health Informatics

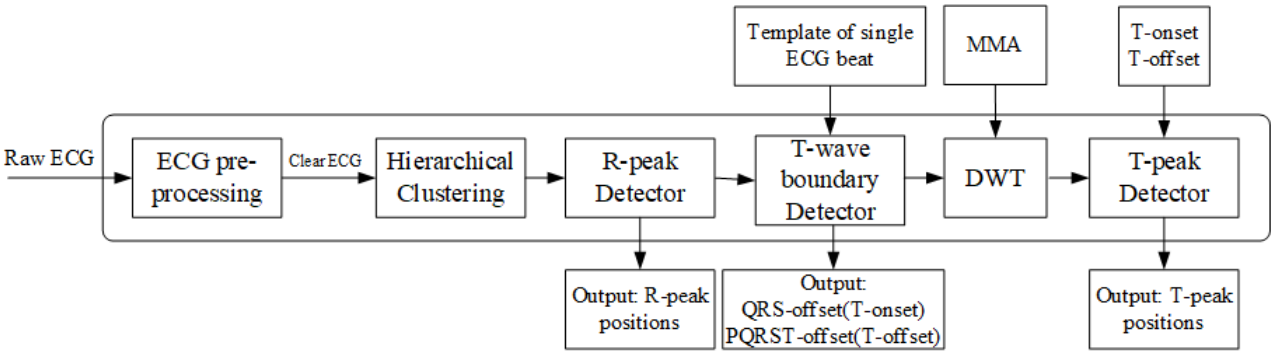

Fig. 1. The system overview of the proposed algorithm

R-peaks. Then, the T-wave boundaries are determined using an ECG template. Finally, the discrete wavelet transform is applied to obtain the DWT coefficients of the T waves, and the MMA method is employed to detect the T-peaks. The flow chart of our proposed algorithm is shown in Fig.1

The rest of the paper is organized as follows: in Section II, we present the theoretical background of the key mathematical methods used in our work. Then we describe our algorithm in Section III and provide the results and the discussion of the validation on MIT-BIH arrhythmia and QT databases in Section IV. Finally, the conclusions are drawn in Section V.

II. THEORETICAL BACKGROUND

A. Hierarchical clustering

Hierarchical clustering is a common machine learning algorithm that seeks to determine the hierarchy of all clusters by analyzing similarity or dissimilarity between pairs of points and has been used for solving a range of physical problems, such as identification of the environment characteristics [26] and statistical analysis of gene expression [27]. Normally, the process of hierarchical clustering is divided into three steps; (1) choose the hierarchical method, (2) select a measure of similarity or dissimilarity and (3) select a clustering algorithm [28].

1) Hierarchical methods: The hierarchical method can be divided into two types. First is Agglomerative clustering, where each object represents a single cluster at the beginning. These individual clusters will be combined based on their similarity step by step. In this case, the two most similar clusters are merged into a new cluster. Then, it will combine with another cluster to generate a new cluster and so on. On the contrary, in divisive clustering, all objects are combined into one cluster initially. Then these objects sequentially split up according to their dissimilarity.

2) Select a measure of similarity or dissimilarity: Selecting a measure of similarity and dissimilarity is an important step as this may influence the clustering results. This step is achieved by calculating the distance between pairs of points. In general, there are three different measures of distance. If we consider two objects A and B with their corresponding positions (X_a, Y_a) and (X_b, Y_b),the formulas of Euclidean distance, City-block distance and Chebychev distance measures are (1), (2) and (3) respectively.

$$D_{Euclidean} = \sqrt{(X_b - X_a)^2 + (Y_b - Y_a)^2} \tag{1}$$

$$D_{City-block} = |(X_b - X_a) + (Y_b - Y_a)| \tag{2}$$

$$D_{Chebychev} = max(|X_b - X_a|, |Y_b - Y_a|) \tag{3}$$

3) Select a clustering algorithm: After choosing the measure of similarity or dissimilarity, the next step is to determine which clustering algorithm will be applied. The most common agglomerative hierarchical clustering algorithms are single linkage algorithm, complete linkage algorithm and average linkage algorithm [29]. Single linkage and complete linkage determine the distance between two clusters based on the shortest and longest path between any two points in these two clusters respectively. However, because the single and complete linkage algorithms are associated with the shortest and longest distance, it may cause one cluster containing a large number of objects and some other small clusters. Average linkage algorithm is used in order to avoid this situation. It can produce clusters with similar sizes based on the average distance between all pairs of points in two clusters. The descriptions of three linkage algorithms are shown in (4), (5) and (6) respectively. The cluster r and s are comprised of the previous clusters, n_r and n_s are the number of objects in cluster r and s respectively. x_{ri} and x_{sj} are the i^{th} and j^{th} object in cluster r and s respectively.

$$\begin{aligned} Linkage_{single}(r,s) &= min(D(x_{ri}, x_{sj})) \\ i &\in (1, \cdots, n_r), j \in (1, \cdots, n_s) \end{aligned} \tag{4}$$

$$\begin{aligned} Linkage_{complete}(r,s) &= max(D(x_{ri}, x_{sj})) \\ i &\in (1, \cdots, n_r), j \in (1, \cdots, n_s) \end{aligned} \tag{5}$$

$$Linkage_{average}(r,s) = \frac{1}{n_r n_s} \sum_{i=1}^{n_r} \sum_{j=1}^{n_s} D(x_{ri}, x_{sj}) \tag{6}$$

B. Discrete wavelet transform

The DWT decomposition is implemented as high and low pass filters, which can obtain the detail (D_x) and approximation (A_x) coefficients in the 2^x scale respectively. The low pass filter removes all the frequency components of the above half of the maximum frequency of the input signal, on the other hand, the high pass removes the components

This article has been accepted for publication in a future issue of this journal, but has not been fully edited. Content may change prior to final publication. Citation information: DOI 10.1109/JBHI.2020.2973982, IEEE Journal of Biomedical and Health Informatics

below half the maximum frequency. However, since half of the frequencies of the input signal have been removed, half the samples can be discarded according to the Nyquists rule. Down sampling is performed after filtering in order to remove half of the samples. The output of the low pass filter will be considered as the input for next level processing. The process is repeated until the desired level of decomposition of the signal is reached. The frequency resolution increases in higher resolution scales, thus low frequency components are more easily detectable in high resolution scales and vice versa. As an example 3-level DWT decomposition is shown in Fig.2. LP and HP stand for low-pass and high pass filters respectively. At each decomposition level n, detail DWT coefficient D_n and approximation coefficient A_n are produced after filtering and down sampling, which can be given in (7).

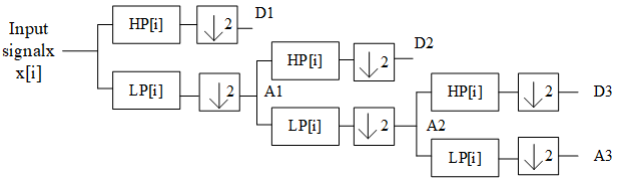

Fig. 2. A level 3 DWT decomposition

$$D_n[i] = \sum_{k=-\infty}^{\infty} D_{n-1}[i] \cdot HP[2i-k]$$
$$A_n[i] = \sum_{k=-\infty}^{\infty} A_{n-1}[i] \cdot LP[2i-k] \quad (7)$$

As the frequency resolution increases in higher resolution scales [8], low frequency components of ECG, such as P and T waves are more easily detectable at higher resolution scales. In this work, the detail coefficients (D4) in 2^4 scale and (D5) in 2^5 scale are used to detect T wave. Once DWT coefficients are computed, MMA will be applied in order to detect the peaks of T wave. At 2^4 and 2^5 resolution level if the value of the detailed DWT coefficients are positive followed by negative, the T-peak is the minimum(convex) point in original ECG data and the vice versa.

III. METHODOLOGY

In this section, we will present the proposed method based on the combination of hierarchical clustering and DWT. Our algorithm aims at detection of QRS complexes and T peaks from the sequence of successive ECG signals. In this work, in order to analyse at least one R-peak and at most two R-peaks each step, we set a sliding time window of $1.2s$ at each step, as we experimentally found out that this is the optimal time window for detecting the R-peaks. Our proposed technique is structured as a four-stage process. First is ECG pre-processing. Raw ECG signals were filtered using fourth-order Butterworth high-pass filter and low-pass filter with the corresponding cut-off frequency of 1 Hz and 30 Hz to remove the noise and baseline wandering [30]. After that, the ECG signal was normalized using (8) so that all the values will be in the range [0,1]. An example can be seen in Fig.3. The

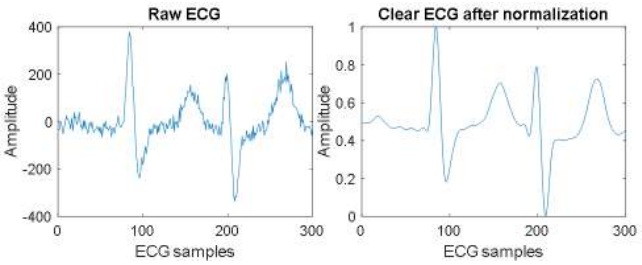

Fig. 3. An example of ECG pre-processing(annotation:se1891m from QT database. The sampling frequency is $250Hz$ hence a time window has 300 ECG samples)

second stage is using hierarchical clustering to determine the R-clusters and non-R clusters, then, identify the R-peaks from R-clusters. The third stage pertains to the T-wave boundary detection based on the R-peak and an ECG period template. The final stage is to find the T-peaks by using DWT and MMA.

$$\widetilde{E}(n) = (E(n) - E_{min}) / (E_{max} - E_{min}) \quad (8)$$

A. Detection of R peak

The strategy of the proposed algorithm is to first identify the R-peak position by using hierarchical clustering. In this stage, we use agglomerative cluster method because we consider every ECG sample as an individual cluster initially and all R wave samples are merged into a cluster based on their similarity. We select Euclidean distance to measure the similarity between each ECG sample. Next, we need to select a clustering method to determine the R-wave clusters. In this case, single and complete linkage algorithms are not applicable because they reduce the assessment of the cluster quality to a single similarity between a pair of objects and they cannot fully reflect the distribution of objects in one cluster. Therefore, they usually produce an undesirable cluster that may include non-R samples. The average linkage algorithm can avoid this situation because it determines the clusters based on the average distance between all pairs of objects. The process of our R-peak detector can be divided into three main stages, namely cluster extraction, R-peak estimation and real R-peak identification. The block diagram of the proposed R-peak detector is drawn in Fig. 4.

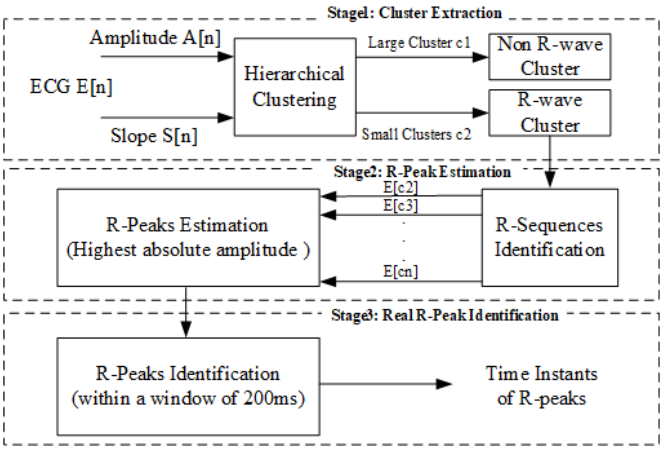

Fig. 4. Flowchart of the proposed R-peak detector

This article has been accepted for publication in a future issue of this journal, but has not been fully edited. Content may change prior to final publication. Citation information: DOI 10.1109/JBHI.2020.2973982, IEEE Journal of Biomedical and Health Informatics

First, for ECG data $E[n]$, each ECG sample $E[i]$ is considered as a individual object with its amplitude $A[i]$ and slope $S[i]$. The slope of an object is defined as the average absolute value of the amplitude difference between $E[i]$ and $E[i+1]$; and $E[i-1]$ respectively. The expression is shown in (9). Then, these objects are considered as the input data to a two-dimensional hierarchical clustering system. The ECG samples are displayed in a two-dimensional coordinate system, with x axis and y axis are the amplitude and slope of each ECG sample respectively as seen on the left of the Fig.5. Then, the hierarchical clustering system will calculate the distance between each object (ECG sample) using (1). Initially, two ECG samples with the shortest distance are merged into a cluster. Then the hierarchical clustering system selects two clusters with the shortest average distance of the ECG samples between them by (6), groups them together into a new cluster and repeats the procedure with the remaining ECG samples. Until the number of cluster become 2, one is a large cluster and another is a small cluster. The cluster with small number of object is R-cluster, since the ECG samples of R-wave is just a small part of the ECG signal. It is shown on the right of the Fig.5, the objects (ECG samples) with relatively larger slope and amplitude are merged into a small cluster, which can be considered as the R-cluster. Other ECG samples are non-R cluster. Here, some of the ECG samples with large amplitude are still considered as non-R cluster, that is because the slope of these objects are relatively low. This is particularly important to solve T-wave oversensing. Even the amplitude of a T-wave is higher than a R-wave, the slope of the T-wave is relatively low. Then the ECG samples of this T-wave will still be grouped into the non-R cluster.

$$S[i] = \begin{cases} |A[i+1] - A[i]| & i = 1, \\ (|A[i+1] - A[i]| + |A[i] - A[i-1]|)/2 & 1 < i < n, \\ |A[i] - A[i-1]| & i = n. \end{cases} \tag{9}$$

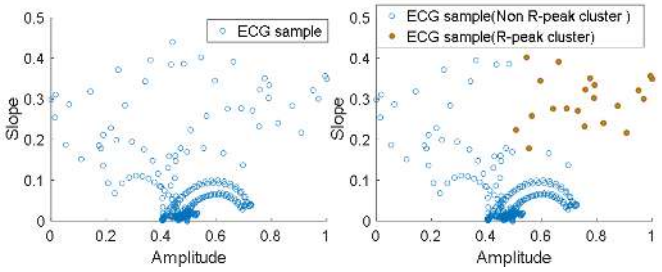

Fig. 5. An example of ECG R-wave cluster extraction based on Fig.3

Once the R-wave clusters are determined in the last stage, the next step is to identify the R-wave ECG sample sequences from these R-wave clusters. As shown on the left of the Fig.6. There are two R-wave sequences (Green points) from the R-peak cluster which are identified using hierarchical clustering. Then, this step is to find the ECG sample with highest absolute value of the amplitude within each R-wave sequences and consider these ECG samples are R-peaks. The final result is shown on the right of the Fig.6.

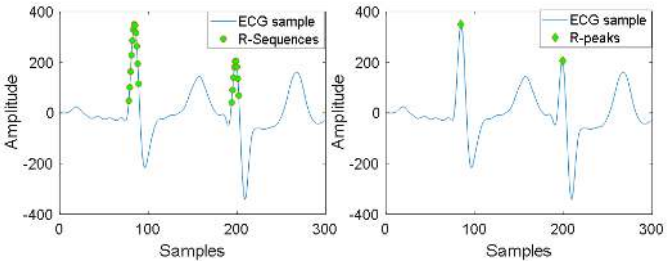

Fig. 6. An example of R-peak Estimation based on Fig.5.

However, there is an abnormal situation that was introduced in [31] named RsR′ pattern. There is an additional spike of QRS complexes caused by any abnormality of conduction in bundle branch block, which is referred to as R′. In addition, as we mentioned earlier, a sliding 1.2 s time window was applied for R-peak detection. In this case, if two successive windows contain half of the same ECG beat, our algorithm will detect two R-peaks that actually are in the same QRS complex. Therefore, a post-processing is needed to remove such R′ peaks from RsR′ pattern or a fake R-peak due to a half ECG beat in a window. We set a threshold of the shortest period between each R peak from two successive QRS complexes, which is from 100 ms [7] to 250 ms [17]. The experimental results showed that 100 ms window is too small if there is a RsR′ pattern in a wide QRS complex and 250 ms is too large to a small QRS complex. From the results, 200 ms time window is an acceptable time window to identify the R-peaks. In this case, if two R-peaks are identified in a window of 200 ms, the one with the lower amplitude is removed and another one is kept as a real R-peak.

B. Determination of the T wave boundary

In this stage, we have the template of a single PQRST period with its corresponding QRS onset, offset and R-peak, which is done by selecting a normal beat with a well-behaved QRS complex that annotated by cardiologists [32]. Fig.7 is an example of a template with the determined QRS complex. The green diamond is marked as R-peak (t_0). Moreover, the PQRST-onset (offset) and QRS-onset (offset) are t_1 (t_2) and t_3 (t_4) respectively. In this case, [t_4,t_2] is considered as T wave boundary of the template. Then we calculated the distance between R-peak and QRS offset, PQRST offset as $t_4 - t_0$ and $t_2 - t_0$ respectively. Once we obtained the R-peak (t_R), the QRS offset(T onset) and PQRST offset (T offset) is initially estimated as $t_{Ton} = t_R + (t_4 - t_0)$ and $t_{Toff} = t_R + (t_2 - t_0)$ respectively. It can be seen in Fig.8, the red points are QRS offset (T onset) and yellow points are PQRST offset (T offset). The next step is to calculate the Mean Square Error (MSE) between ECG samples (E_i) in the T wave boundary of the template and ECG samples ($\tilde{E}_i$) in each estimated T wave boundary using (10), where n is the number of ECG samples in T wave boundary.

$$MSE = \frac{1}{n}\sum_{i=1}^{n}(E_i - \tilde{E}_i)^2 \tag{10}$$

Finally each estimated T wave boundary is moved forward and backward by 20 samples $\tilde{E}_{i\pm 20}$ and the respective MSE is

This article has been accepted for publication in a future issue of this journal, but has not been fully edited. Content may change prior to final publication. Citation information: DOI 10.1109/JBHI.2020.2973982, IEEE Journal of Biomedical and Health Informatics

calculated. The final T wave boundaries are extracted based on the minimum MSE between E_i and $\tilde{E}_{i\pm 20}$. It also need to be noted that our obtained T wave boundaries obtained here may not be the actual T wave boundaries, since once the width of ECG beat become abnormal, such T wave boundaries can not be identified accurately using a normal template. Therefore, the main idea of our algorithm is to determine the approximate range based on the T boundary to make sure the T-peak is in this range.

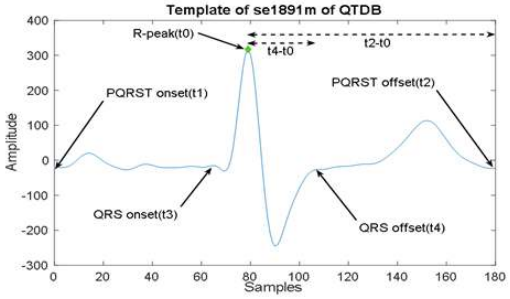

Fig. 7. The template of the single PQRST period (annotation:se1891m from QT database)

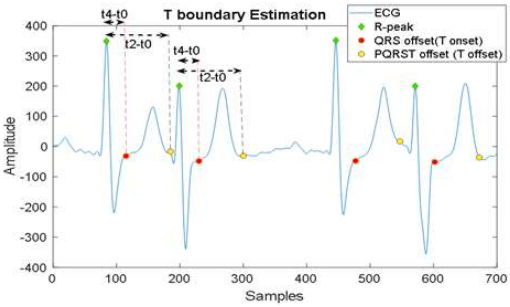

Fig. 8. T wave boundary estimation using template (Fig.7) (annotation:se1891m from QT database)

C. Detection of T peak

Once the approximate T wave boundaries are finalized. DWT is applied to combine with the MMA method to determine the T-peaks. We developed an algorithm that takes inspiration from the work of [5] and [8]. Since the T waves have significant components at higher scale, it is possible to detect T-peaks at scale 2^4 or 2^5 using DWT [5]. In this case, we selected 'Haar' as the wavelet function in order to reduce the computational complexity, because it is the simplest wavelet function and it is sufficient for T-peak detection [8]. In this work, the 2^4 and 2^5 resolution scale detailed coefficients are first determined by using DWT. Once DWT coefficients are computed, the next step is to use MMA to find the positions of T peaks. Given the positive or negative deflection of the T wave, compared to the baseline, the pair of extrema that indicates the waves temporal position can be either a wavelet coefficient with minimum value followed by a maximum wavelet coefficient, for positive deflection or the reverse for a negative deflection. Through MMA, we initially obtain the temporal position by calculating t_1, t_2 with the maximum or minimum values in the D4 coefficients and t_3, t_4 in the D5 coefficients. As mentioned before, half of the samples are discarded at each level after filtering in DWT. Therefore, it is noted that the temporal resolutions on the 2^4 and 2^5 are diminished (by a factor of 16 and 32 respectively) compared to the original timescale. Thus, the T peak time point is calculated as the maximum or minimum of the data within time widows $[t_1 \times 2^4,\ t_2 \times 2^4]$ and $[t_3 \times 2^5,\ t_4 \times 2^5]$. If the deflection detected in the MMA is characterized as negative, then T wave is inverted. The final step is to compare the absolute values of T peak amplitudes, which are obtained from the last step. The one with the highest absolute value of the amplitude is kept as the T peak. A detailed example is shown in Fig.9. Once the T wave boundaries are determined, the DWT is applied to calculate the D4 and D5 coefficients of the T wave. From the D4 coefficients, the t_1 and t_2 are 3 and 5 respectively, the T peak time point is then calculated as the maximum value within the time window $[3 \times 2^4,\ 5 \times 2^4]$. In this case, the T peak time point is identified at 58. On the other side, the T peak time point based on the D5 coefficients within the time window $[2 \times 2^5,\ 3 \times 2^5]$ is calculated at 64. Finally, the real T peak is determined at 58 with amplitude 46.5 rather than another T peak with lower amplitude 38.1. Although it is noted that the T waves have different morphology, such as peaked T waves, inverted T waves, biphasic T waves, T waves with two peaks etc. [33]. The main aim of our system is to identify the T-peak with the largest absolute value of the amplitude as the real T-peaks in each window. Fig.10 is the final result of our algorithm as an example record (se1891) with T wave oversensing problem from QT database. The green diamonds and the red squares are R-peaks and T-peaks respectively.

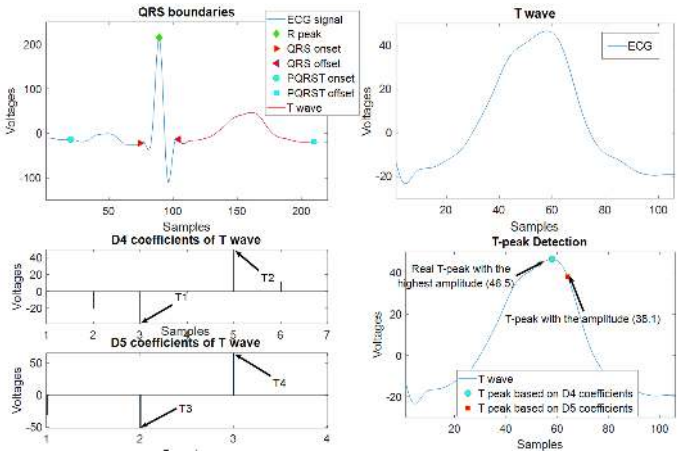

Fig. 9. T peak detection based on DWT and MMA

IV. Results and Discussion

A. Data and Validation

The MIT-BIH and QT databases [32] are used to validate our proposed algorithm. First we used all 48 30-minutes ECG records with 360Hz sampling frequency of MIT-BIH databse. In this work, we calculated sensitivity $Se = TP/(TP+FN)$, positive predictivity $+P = TP/(TP + FP)$ and Accuracy $Acc = TP/(TP + FP + FN)$ of the annotated R wave

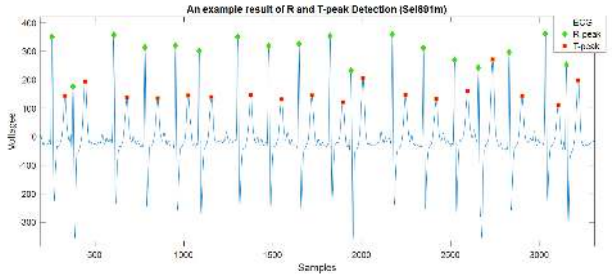

Fig. 10. The result of an example with T wave oversensing for R and T peak Detection.(annotation:sel891m)

peaks, where TP is the true positives (peak is detected of the annotated peak), FN denotes the false negatives (annotated peak is not detected) and FP is the false positives (when peak is detected outside the range of the annotated peak). In this work, we calculated sensitivity Se and positive predictivity $+P$ by considering the range of 150ms ($\pm$75ms) of the annotated R-peaks based on the AAMI-ECAR guidelines [34] in order to compare with the literature under the same condition. We compared the performance of our algorithm with other established algorithm for R-peak detection, which is shown in Table I. Table II shows the effectiveness of our R-peak detector in terms of false positives. For the QT database, it has 105 2-lead recordings with a sampling frequency of 250Hz. It includes different T wave morphologies, such as normal, inverted, only upwards and only downwards deflections [35]. In this work, all ECG records (more than 111200 beats) of the automatically annotated QT database is used to evaluate our algorithm. Moreover, the 103 manually annotated records of Lead I are also used since they are more salient. The results are finally compared with other methods.

We also evaluated the detection accuracy of our algorithm based on the time difference (error) between the detected peaks and the manual annotated peaks. The accuracy in terms of the average of the errors (m) and the standard deviation (s) of the errors are obtained for all the records. The results and the comparison with the literature are given in Table III. Finally, we built a record-by-record classification as proposed in [5] and more recently in [17] for T peak detection. We chose the same threshold in [5] to compare with the previous works. The thresholds are measured by the 15ms for the absolute average error ($bias$) and 30.6ms for the standard deviation (s). Thus, these records are divided into four groups based on the following rule: Group I: $bias < 15ms$ and $s < 30.6ms$; Group II: $bias > 15ms$ and $s < 30.6ms$; Group III: $bias < 15ms$ and $s > 30.6ms$ and Group IV: $bias > 15ms$ and $s > 30.6ms$. The comparison results with three established algorithms for the T peak detection are shown in Table IV.

B. Method Evaluation

The proposed algorithm shows the high performance in the delineation of ECG R and T-peaks. Concerning the R peak detection, the Table I shows our method achieves 99.89% Se, 99.94% $+P$ and 99.83% Acc for R-peak detection. The performance in terms of $+P$ and Acc is higher than other previously proposed works. From Table II, it can be seen in our work, false positives of R-peak detection can be effectively reduced and only exist in the records with baseline drifts. In the future work, the performance of our algorithm can be improved with the removal of baseline drifts in such ECG records. Furthermore, Table III shows that for R peak detection, this algorithm achieves 100% Se and 99.83% $+P$ over the manually annotated QT database. It also achieved a Se of 99.92% and a $+P$ of 99.96% over the automatically annotated QT database. Although three studies in literature [18], [7] and [14] achieved slightly higher Se for R-peak detection, the number of true positive of our algorithm for R-peak detection is larger than these studies. Overall, the R-peak detection performance of our algorithm is generally better or comparable with the previous work.

In terms of the T-peak detection in manually annotated QT database, our algorithm achieved a Se of 99.91% and a $+P$ of 99.38%. Although we used a 150 ms window to define the true positive of T-peak detection, the mean (m) and standard deviation (s) of errors are lower than most of the previous work. It is also noted that the study in literature [18] achieved lower mean (m) and standard deviation (s) of errors for T-peak detection. However, they did not annotate the number of the true positives and this may reflect they did not use all manual annoted QT database. Moreover, the QT database stratification based on the T peak detection is given in Table IV. It shows that the T peaks in the 95% of the records were detected by our method, which is higher than other referenced methods. The other 5% records in Group III and IV show the larger mean (m) and standard deviation (s) than other works. This might be the reason for causing large mean (m) and standard deviation (s) of errors over the whole QT databse. A deeper analysis shows the records in these two groups are from "sudden death" patients which can be checked in [35]. Our method may have problems in T peak detection for "sudden death" records because the morphology of T waves in these records may be erratic. Further study is needed to investigate this type of condition.

V. Conclusion

In this paper, we have proposed a new algorithm based on the hierarchical clustering and discrete wavelet transform for the automatic delineation of the ECG fiducial points (R and T peaks)[1]. The use of hierarchical clustering allows for identifying the R clusters and determining the R peaks with high accuracy. The combination of DWT and MMA analysis help us to detect the T peaks with high sensitivity. Our algorithm has been validated on the MIT-BIH arrhythmia database and QT database. The results show that our algorithm can solve T-wave oversensing problem and effectively reduce the number of R-peak false-positive detection. Moreover, the performance of algorithm is generally better than other referenced algorithms.

[1]A detailed detection performance of our proposed algorithm for each record can be found in https://drive.google.com/file/d/1wuhDQ7fKUTVQa8PQmFBt3E_DSaItfDIr/view?usp=sharing

This article has been accepted for publication in a future issue of this journal, but has not been fully edited. Content may change prior to final publication. Citation information: DOI 10.1109/JBHI.2020.2973982, IEEE Journal of Biomedical and Health Informatics

TABLE I
THE R-PEAK (QRS) DETECTION PERFORMANCE COMPARISON IN THE MIT-BIH ARRHYTHMIA DATABASE.(THE WINDOW USED FOR DEFINING A TRUE POSITIVE IS REPORTED AS w, N/R: NOT REPORTED)

Authors	Method Used	w[ms]	TP	FP	FN	Se[%]	+P[%]	Acc[%]
This work	**Hierarchical clustering**	**150**	**109370**	**63**	**124**	**99.89**	**99.94**	**99.83**
Martinez et al. [5]	Wavelet transform(WT)	N/R	109208	153	220	99.80	99.86	99.66
Ghaffari et al. [18]	Discrete wavelet transform(DWT)	150	109327	129	101	99.91	99.88	99.79
Manikandan et al. [7]	Shannon energy envelope(SEE)	N/R	109356	140	79	99.93	99.86	99.79
Elgendi et al. [16]	Moving average filters	N/R	N/R	N/R	N/R	99.78	99.87	N/R
Merah et al. [9]	Stationary wavelet transform(SWT)	100	109316	126	178	99.84	99.88	99.72
Saadi et al. [14]	Optimized adaptive thresholding	150	N/R	N/R	N/R	99.90	99.87	N/R
Thiamchoo et al. [10]	Continuous wavelet transform(CWT)	N/R	109135	356	185	99.69	99.83	99.52
Thungtong [11]	Discrete wavelet transform(DWT)	N/R	109096	242	409	99.63	99.78	99.41
Smaoui et al. [12]	Continuous wavelet transform(CWT)	N/R	N/R	168	756	99.37	99.83	N/R
Cesari et al. [17]	Wavelet transform (WT)	150	109321	147	173	99.84	99.87	99.71
Friganovic et al. [23]	Mathematical morphological filter	150	98659	268	214	99.78	99.72	99.52
Zalabarria et al. [15]	Iterative state machines	N/R	106096	431	485	99.54	99.60	N/R

TABLE II
COMPARISON OF THE NUMBERS OF FALSE-POSITIVES (FPS) BASED ON R-PEAK DETECTION FOR SPECIFIC RECORDS OF THE MIT-BIH ARRYTHMIA DATABASE, (WHERE **N/A** IS NOISE AND ARTEFACT, **BD** IS BASELINE DRIFTS, **IR** IS IRREGULAR RHYTHMIC, **VA** IS VENTRICULAR ARRHYTHMIAS, **SCR** IS SUDDEN CHANGES IN R-PEAK, **HT** AND **HP** ARE HIGH T-PEAK AND P-PEAK RESPECTIVELY, **PVCS** IS PREMATURE VENTRICULAR CONTRACTIONS AND **SQRS** IS SMALL QRS COMPLEXES.)

No.	Characteristics	Number of false-positive (FP) detection						
		Ref. [7]	Ref. [9]	Ref. [10]	Ref. [11]	Ref. [12]	Ref. [15]	**This work**
104	N/A	14	12	15	7	32	3	**0**
105	N/A	18	11	22	48	25	9	**0**
108	N/A, BD, HP	12	10	12	40	19	73	**5**
113	HT	3	4	8	4	0	0	**0**
116	BD, sQRS	8	7	2	26	2	1	**10**
200	N/A, VA	6	0	16	6	7	0	**0**
203	N/A, BD, IR, VA	5	10	14	53	24	24	**10**
208	BD, PVCs, sQRS	5	3	4	22	4	4	**7**
210	N/A, BD	3	3	3	16	4	1	**7**
222	BD, IR, HP	0	5	1	4	1	0	**4**
223	SCR	0	0	1	8	0	0	**0**
228	N/A, BD	7	7	19	5	19	9	**7**
232	BD	18	10	4	2	2	12	**4**
233	VA	0	0	0	13	0	0	**0**
Total		99	82	121	254	139	136	**54**

TABLE III
R-PEAK (QRS) AND T-PEAK DETECTION PERFORMANCE COMPARISON IN THE QT DATABASE.(THE WINDOW USED FOR DEFINING A TRUE POSITIVE IS REPORTED AS w, N/R: NOT REPORTED)

	Authors	Method Used	Annotation(File Name)	w[ms]	TP	FP	FN	Se[%]	+P[%]	Acc[%]
R-peak (QRS)	**This work**	**Hierarchical clustering**	**Manual(.qlc)**	**150**	**3617**	**6**	**0**	**100**	**99.83**	**99.83**
	Martinez et al. [20]	Phasor transform	Manual(.qlc)	N/R	N/R	N/R	N/R	99.85	N/R	N/R
	Cesari et al. [17]	WT	Manual(.qlc)	150	N/R	N/R	N/R	100	N/R	N/R
	This work	**Hierarchical clustering**	**Automatic(.pu)**	**150**	**111153**	**47**	**91**	**99.92**	**99.96**	**99.88**
	Martinez et al. [5]	WT	Automatic(.pu)	N/R	86824	107	68	99.92	99.88	99.80
	Ghaffari et al. [18]	DWT	Automatic(.pu)	150	86845	79	47	99.94	99.91	99.85
	Elgendi et al. [16]	Moving average filters	Automatic(.pu)	N/R	110834	N/R	N/R	99.99	99.67	N/R
	Merah et al. [9]	SWT	Automatic(.pu)	100	86837	99	55	99.94	99.89	99.82
	Thungtong [11]	DWT	Automatic(.pu)	N/R	83092	80	206	99.75	99.90	99.66
	Friganovic et al. [23]	Mathematical morphological filter	Automatic(.pu)	150	84849	2161	1508	98.25	97.51	95.76
	Authors	Method Used	Annotation(File Name)	w[ms]	TP	FP	FN	Se[%]	+P[%]	m±s(ms)
T-peak	**This work**	**Hierarchical clustering and DWT**	**Manual(.qlc)**	**150**	**3520**	**22**	**3**	**99.91**	**99.38**	**1.4±8.2**
	Martinez et al. [5]	WT	Manual(.qlc)	N/R	N/R	N/R	N/R	99.77	97.79	0.2±13.9
	Ghaffari et al. [18]	DWT	Manual(.qlc)	N/R	N/R	N/R	N/R	99.87	99.80	0.3±4.1
	Martinez et al. [20]	Phasor transform	Manual(.qlc)	N/R	N/R	N/R	N/R	99.20	N/R	5.3±12.9
	Elgendi et al. [21]	Moving average filters	Manual(.qlc)	60	N/R	N/R	N/R	98.90	98.77	N/R
	Cesari et al. [17]	WT	Manual(.qlc)	150	N/R	N/R	N/R	99.50	N/R	-2.6±12.2
	Friganovic et al. [23]	WT+templates	Manual(.qlc)	160	3115	464	427	87.94	87.03	N/R

TABLE IV
QT DATABASE STRATIFICATION ACCORDING TO THE T-PEAK DETECTION.(N/A: NOT AVAILABLE)

QT databse	Group I		Group II		Group III		Group IV	
Method	%	m±s[ms]	%	m±s[ms]	%	m±s[ms]	%	m±s[ms]
This work	**95**	**2.86±5.62**	**0**	**N/A**	**2**	**12.07±54.53**	**3**	**33.13±74.02**
Ref. [5]	83	3.9±7.6	5	-2.7±17	5	-0.5±37	7	-42±72
Ref. [17]	89	-5.5±7.7	2	8.7±22.5	3	-3.1±55.3	6	38.1±50.5
Ref. [36]	82	4.2±8.6	8	36±15	4	9.6±38	6	32±40

REFERENCES

[1] W.H.O., "Cardiovascular diseases (cvds)," 2019. [Online]. Available: https://www.who.int/cardiovascular_diseases/en/

[2] C.-T. Lin, K.-C. Chang, C.-L. Lin, C.-C. Chiang, S.-W. Lu, S.-S. Chang, B.-S. Lin, H.-Y. Liang, R.-J. Chen, Y.-T. Lee *et al.*, "An intelligent telecardiology system using a wearable and wireless ecg to detect atrial fibrillation," *IEEE Transactions on Information Technology in Biomedicine*, vol. 14, no. 3, pp. 726–733, 2010.

[3] S.-N. Yu and M.-Y. Lee, "Bispectral analysis and genetic algorithm for congestive heart failure recognition based on heart rate variability," *Computers in Biology and Medicine*, vol. 42, no. 8, pp. 816–825, 2012.

[4] Ö. Yıldırım, P. Pławiak, R.-S. Tan, and U. R. Acharya, "Arrhythmia detection using deep convolutional neural network with long duration ecg signals," *Computers in biology and medicine*, vol. 102, pp. 411–420, 2018.

[5] J. P. Martínez, R. Almeida, S. Olmos, A. P. Rocha, and P. Laguna, "A wavelet-based ecg delineator: evaluation on standard databases," *IEEE Transactions on biomedical engineering*, vol. 51, no. 4, pp. 570–581, 2004.

[6] J. Pan and W. J. Tompkins, "A real-time qrs detection algorithm," *IEEE Trans. Biomed. Eng*, vol. 32, no. 3, pp. 230–236, 1985.

[7] M. S. Manikandan and K. Soman, "A novel method for detecting r-peaks in electrocardiogram (ecg) signal," *Biomedical Signal Processing and Control*, vol. 7, no. 2, pp. 118–128, 2012.

[8] E. B. Mazomenos, D. Biswas, A. Acharyya, T. Chen, K. Maharatna, J. Rosengarten, J. Morgan, and N. Curzen, "A low-complexity ecg feature extraction algorithm for mobile healthcare applications," *IEEE journal of biomedical and health informatics*, vol. 17, no. 2, pp. 459–469, 2013.

[9] M. Merah, T. Abdelmalik, and B. Larbi, "R-peaks detection based on stationary wavelet transform," *Computer methods and programs in biomedicine*, vol. 121, no. 3, pp. 149–160, 2015.

[10] N. Thiamchoo and P. Phukpattaranont, "R peak detection algorithm based on continuous wavelet transform and shannon energy," *ECTI Transactions on Computer and Information Technology (ECTI-CIT)*, vol. 10, no. 2, pp. 167–175, 2016.

[11] A. Thungtong, "A robust algorithm for r peak detection based on optimal discrete wavelet transform," in *2017 14th International Joint Conference on Computer Science and Software Engineering (JCSSE)*. IEEE, 2017, pp. 1–6.

[12] G. Smaoui, A. Young, and M. Abid, "Single scale cwt algorithm for ecg beat detection for a portable monitoring system," *Journal of Medical and Biological Engineering*, vol. 37, no. 1, pp. 132–139, 2017.

[13] Z. Hou, Y. Dong, J. Xiang, X. Li, and B. Yang, "A real-time qrs detection method based on phase portraits and box-scoring calculation," *IEEE Sensors Journal*, vol. 18, no. 9, pp. 3694–3702, 2018.

[14] D. B. Saadi, G. Tanev, M. Flintrup, A. Osmanagic, K. Egstrup, K. Hoppe, P. Jennum, J. L. Jeppesen, H. K. Iversen, and H. B. Sorensen, "Automatic real-time embedded qrs complex detection for a novel patch-type electrocardiogram recorder," *IEEE journal of translational engineering in health and medicine*, vol. 3, pp. 1–12, 2015.

[15] U. Zalabarria, E. Irigoyen, R. Martinez, and A. Lowe, "Online robust r-peaks detection in noisy electrocardiograms using a novel iterative smart processing algorithm," *Applied Mathematics and Computation*, vol. 369, p. 124839, 2020.

[16] M. Elgendi, "Fast qrs detection with an optimized knowledge-based method: Evaluation on 11 standard ecg databases," *PloS one*, vol. 8, no. 9, p. e73557, 2013.

[17] M. Cesari, J. Mehlsen, A.-B. Mehlsen, and H. B. D. Sorensen, "A new wavelet-based ecg delineator for the evaluation of the ventricular innervation," *IEEE journal of translational engineering in health and medicine*, vol. 5, pp. 1–15, 2017.

[18] A. Ghaffari, M. Homaeinezhad, M. Akraminia, M. Atarod, and M. Daevaeiha, "A robust wavelet-based multi-lead electrocardiogram delineation algorithm," *Medical engineering & physics*, vol. 31, no. 10, pp. 1219–1227, 2009.

[19] G. de Lannoy, B. Frénay, M. Verleysen, and J. Delbeke, "Supervised ecg delineation using the wavelet transform and hidden markov models," in *4th European Conference of the International Federation for Medical and Biological Engineering*. Springer, 2009, pp. 22–25.

[20] A. Martínez, R. Alcaraz, and J. J. Rieta, "A new method for automatic delineation of ecg fiducial points based on the phasor transform," in *2010 Annual International Conference of the IEEE Engineering in Medicine and Biology*. IEEE, 2010, pp. 4586–4589.

[21] M. Elgendi, B. Eskofier, and D. Abbott, "Fast t wave detection calibrated by clinical knowledge with annotation of p and t waves," *Sensors*, vol. 15, no. 7, pp. 17 693–17 714, 2015.

[22] M. Elgendi, M. Meo, and D. Abbott, "A proof-of-concept study: Simple and effective detection of p and t waves in arrhythmic ecg signals," *Bioengineering*, vol. 3, no. 4, p. 26, 2016.

[23] K. Friganovic, D. Kukolja, A. Jovic, M. Cifrek, and G. Krstacic, "Optimizing the detection of characteristic waves in ecg based on processing methods combinations," *IEEE access*, vol. 6, pp. 50 609–50 626, 2018.

[24] M. R. Homaeinezhad, M. ErfanianMoshiri-Nejad, and H. Naseri, "A correlation analysis-based detection and delineation of ecg characteristic events using template waveforms extracted by ensemble averaging of clustered heart cycles," *Computers in biology and medicine*, vol. 44, pp. 66–75, 2014.

[25] M. Yochum, C. Renaud, and S. Jacquir, "Automatic detection of p, qrs and t patterns in 12 leads ecg signal based on cwt," *Biomedical Signal Processing and Control*, vol. 25, pp. 46–52, 2016.

[26] S. Bandyopadhyay and E. J. Coyle, "An energy efficient hierarchical clustering algorithm for wireless sensor networks," in *IEEE INFOCOM 2003. Twenty-second Annual Joint Conference of the IEEE Computer and Communications Societies (IEEE Cat. No. 03CH37428)*, vol. 3. IEEE, 2003, pp. 1713–1723.

[27] N. A. Heard, C. C. Holmes, and D. A. Stephens, "A quantitative study of gene regulation involved in the immune response of anopheline mosquitoes: An application of bayesian hierarchical clustering of curves," *Journal of the American Statistical Association*, vol. 101, no. 473, pp. 18–29, 2006.

[28] M. Sarstedt, E. Mooi *et al.*, "A concise guide to market research," *The Process, Data, and*, 2014.

[29] O. A. Abbas, "Comparisons between data clustering algorithms." *International Arab Journal of Information Technology (IAJIT)*, vol. 5, no. 3, 2008.

[30] A. Amann, R. Tratnig, and K. Unterkofler, "Reliability of old and new ventricular fibrillation detection algorithms for automated external defibrillators," *Biomedical engineering online*, vol. 4, no. 1, p. 60, 2005.

[31] S. Maheshwari, A. Acharyya, P. E. Puddu, E. B. Mazomenos, G. Leekha, K. Maharatna, and M. Schiariti, "An automated algorithm for online detection of fragmented qrs and identification of its various morphologies," *Journal of The Royal Society Interface*, vol. 10, no. 89, p. 20130761, 2013.

[32] A. L. Goldberger, L. A. Amaral, L. Glass, J. M. Hausdorff, P. C. Ivanov, R. G. Mark, J. E. Mietus, G. B. Moody, C.-K. Peng, and H. E. Stanley, "Physiobank, physiotoolkit, and physionet: components of a new research resource for complex physiologic signals," *Circulation*, vol. 101, no. 23, pp. e215–e220, 2000.

[33] E. Burns, "Ecg library," 2019. [Online]. Available: https://litfl.com/t-wave-ecg-library/

[34] A. ECAR, "Recommended practice for testing and reporting performance results of ventricular arrhythmia detection algorithms," *Association for the Advancement of Medical Instrumentation*, p. 69, 1987.

[35] P. Laguna, R. G. Mark, A. Goldberg, and G. B. Moody, "A database for evaluation of algorithms for measurement of qt and other waveform intervals in the ecg," in *Computers in Cardiology 1997*. IEEE, 1997, pp. 673–676.

[36] J. A. Vila, Y. Gang, J. M. R. Presedo, M. Fernández-Delgado, S. Barro, and M. Malik, "A new approach for tu complex characterization," *IEEE Transactions on Biomedical Engineering*, vol. 47, no. 6, pp. 764–772, 2000.